16th Australasian Fluid Mechanics Conference
Crown Plaza, Gold Coast, Australia
2-7 December 2007

Interferometric detection of dispersed shock waves in small scale diaphragm-less shock tube of 1mm diameter

S. Udagawa[1] and W. Garen[2] and B. Meyerer[2] and K. Maeno[3]

[1]Graduate School of Science and Technology
Chiba University, Chiba, 263-8522 JAPAN

[2]Department of Photonics
University of Applied Science, Oldenburg/Ostfriesland/Wilhelmshaven, Emden, 26723 GERMANY

[3]Graduate School of Engineering
Chiba University, Chiba, 263-8522 JAPAN

Abstract

We have developed a small scale shock tube of 1mm diameter which has a diaphragm-less driver section. The experiment is performed by using our small scale shock tube, where the propagation velocities of the shock waves are measured with a specially designed laser interferometer under several pressure conditions. Helium and CO_2 are used as the driver and test gas, respectively. As the results show, we have succeeded in observing weak shock waves in a shock tube of 1mm diameter. The fully or partly dispersed shock waves, which are attributed to the exitation of the vibrational energy of CO_2, are also observed at the weak shock region.

Introduction

Recently, the micro-shock wave has come to the attention of researchers in several fields of science. The diffusive transport phenomena, such as heat conduction with the wall and the shear stress, lead to remarkable deviation from the ideal shock behavior in a narrow channel, which was described by Brouillette[1]. The scaling parameter S is expressed as following equation.

$$S = \frac{Re \cdot D}{4L} \tag{1}$$

Here, Re and D are the Reynolds number and the diameter of the shock tube, and L is the distance between the shock wave and the contact surface of the driver and test gases. The formula of the Hugoniot curve for the density ratio across a shock wave can be expressed as follows:

$$\frac{\rho_2}{\rho_1} = \frac{(\gamma_1+1)M^2 + \frac{2\gamma_1 M}{Pr}\cdot\frac{1}{S} + \left(\frac{1}{S}\right)^2 \frac{2\gamma_1}{Pr}}{(\gamma_1-1)M^2 + \frac{1}{S}\cdot\frac{2}{M\cdot Pr} + 2} \tag{2}$$

If S becomes infinite, the well known ideal density ratio can be derived:

$$\frac{\rho_2}{\rho_1} = \frac{(\gamma_1+1)M^2}{(\gamma_1-1)M^2+2} \tag{3}$$

Shock waves at micro scales may be of high potentiality for further scientific applications. Garen et al.[2] performed shock wave measurements by using the uniquely developed diaphragm-less driver section with a specially designed laser differential interferometer, in a shock tube of 3mm diameter. It is also shown experimentally that the Mach number of the shock wave depends on the Reynolds number. It is no longer only a function of the initial pressure ratio across the quickly opening valve p_4/p_1, but also is strongly correlated to the Reynolds number in the narrow channel[2]. The diaphragm-less driver section and the laser differential interferometer are highly suitable for generating and measuring the shock wave propagation in a small diameter tube.

In addition, catching the shock waves and the contact surfaces along the axial direction is of great importance. First, we have performed a detailed experiment under the same pressure conditions at several different positions in a shock tube of 3mm diameter by using the diaphragm-less driver section and the laser differential interferometer which are developed by Garen et al.[2]. Secondly, we have performed a numerical simulation in comparison with the experimental results[3]. Furthermore, we have progressed in weak shock wave measurements in a shock tube of 1mm diameter by using helium and air as driver and test gas, respectively. It is shown that in the case of a laminar flow behind the shock wave the friction effect between the shock tube wall and the test gas leads to a remarkable behaviour[4]. In this study we have carried out the measurements of weak shock waves in a shock tube of 1mm diameter with the same measuring arrangement by using helium and CO_2 as driver and test gas to detect the dispersed effect of the gas.

Vibrational energy in the CO_2 molecule[5]

The vibrational energy of the carbon dioxide gas molecule at normal temperature has the magnitude which equilibrate with the translational and rotational energy. The vibrational relaxation time of the molecule, which is about 7μs at 300K, is suitable duration for an optical measurement of the dispersed wave in a shock tube. As mentioned above, the carbon dioxide gas is often used for the experimental study of a weak shock wave with vibrational relaxation of the molecule. The structure of the carbon dioxide molecule has the collinear symmetrical shape with four vibrational modes, which consist of the symmetrical stretching mode, two degenerated bending modes, and the asymmetrical stretching mode, as shown in figure 1. The vibra-

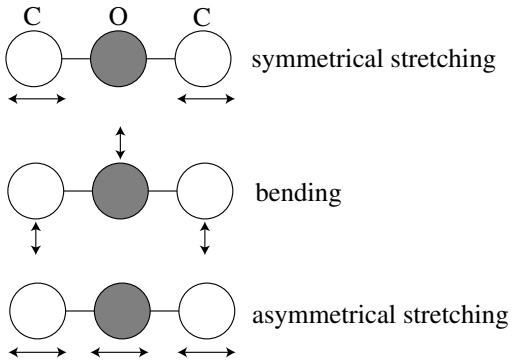

Figure 1: Three vibrational modes of carbon dioxide

tional specific heat for each vibrational mode C_{vib,ν_n} is denoted

as follows, if the harmonic oscillator of the vibration is assumed for molecular vibration.

$$C_{vib,\nu_1} = \frac{(\frac{\theta_{\nu_1}}{T})^2 exp(\frac{\theta_{\nu_1}}{T})}{[exp(\frac{\theta_{\nu_1}}{T})-1]^2} R \tag{4}$$

$$C_{vib,\nu_2} = \frac{2(\frac{\theta_{\nu_2}}{T})^2 exp(\frac{\theta_{\nu_2}}{T})}{[exp(\frac{\theta_{\nu_2}}{T})-1]^2} R \tag{5}$$

$$C_{vib,\nu_3} = \frac{(\frac{\theta_{\nu_3}}{T})^2 exp(\frac{\theta_{\nu_3}}{T})}{[exp(\frac{\theta_{\nu_3}}{T})-1]^2} R \tag{6}$$

Here, θ_{ν_1}, θ_{ν_2} and θ_{ν_3} are called the vibrational characteristic temperatures, which have the values of 1999K, 960K and 3383K. The vibrational specific heat fraction for ν_1, ν_2 and ν_3 modes at 273K is shown as follows:

$$C_{vib,\nu_1} : C_{vib,\nu_2} : C_{vib,\nu_3} = 0.046 : 1 : 0.0008 \tag{7}$$

In this study ν_1 and ν_2 are considered as the vibrational modes for carbon dioxide gas molecule as follows:

$$C_{vib} = C_{vib,\nu_1} + C_{vib,\nu_2} \tag{8}$$

Structure of the dispersed wave[5]

The dissipation by the molecular vibrational non-equilibrium is the dominant effect for a smoothing of a weak shock wave surface structure, in particular for the polyatomic molecule. The thickness of the wave front increases to dozens of times of thickness of the normal shock wave front, or several hundred times, by considering the translational-vibrational non-equilibrium of the molecule. In this study the dissipation effect is considered only as the vibrational non-equilibrium effect of the molecule. Generally, the velocity of the sound wave, which propagates in the polyatomic molecular gas, depends on the wave frequency. In the case of a very high frequency sound wave, the vibrational mode of the molecule can not follow the sudden change of state. Consequently, the wave propagates by freezing the vibrational energy. The sound velocity with the frozen vibrational energy, which is called frozen sound velocity a_f, is denoted as the following equation:

$$a_f = \sqrt{\gamma_f RT} \tag{9}$$

Here, R is a gas constant and γ_f is called frozen specific heat ratio, which has a value of 7/5 for a gas with a diatomic molecular or collinear symmetrical molecular structures. On the other hand, in the case of a very low frequency sound wave, the vibrational mode of the molecule is excited keeping equilibrium with translational and rotational modes because of a gradual change of state in the gas. In this case the sound velocity, called equilibrium sound velocity a_e, is denoted as the following equation:

$$a_e = \sqrt{\gamma_e RT} \tag{10}$$

Here, γ_e is equilibrium specific heat ratio, which is denoted as follows:

$$\gamma_e = \frac{\frac{7}{2}R + C_{vib}}{\frac{5}{2}R + C_{vib}} \tag{11}$$

The relation such as $a_f > a_e$ has been derived from the equations (9) to (11). When a weak shock wave, which propagates in the polyatomic molecular gas, passes into the gas with the structure of a steady wave front, it is caused by the equilibrium between the non-linear effect of the compression wave and the dissipative effect of the molecule. In the case of a weak shock wave, the continuous profile is obtained throughout the wave front because the vibrational non-equilibrium effect is dominant. In a strong shock wave, the vibrational modes in the molecules across the front of the wave, can not follow the sudden change of state, caused by the non-linear effect of the pressure wave. Consequently, the wave propagates by freezing the vibrational energy. On the other hand, the non-linear effect keeps equilibrium between the translational and the rotational relaxation effects of the molecule. Such a wave front has a very thin and discontinuous structure, caused by the translational and rotational equilibrium energies of the molecule and by several intermolecular collisions. The wave front with a relatively thick and continuous profile is generated by the vibrational non-equilibrium effect behind the discontinuous wave front. Generally, such a structure of the weak wave front passes through the transient state until achieving the steady state. As mentioned above, the weak shock wave, which propagates in the polyatomic molecular gas, has a structure corresponding to the high frequency sound wave in front of the wave surface, and for the low frequency sound wave behind the wave front. Here, we consider that the weak shock wave propagates in the stationary polyatomic molecule gas. The velocity of the shock wave meets the following relation:

$$a_e < U_s < a_f \tag{12}$$

The vibrational modes are excited all over the shock wave, and the wave is dispersed and smoothed by the vibrational non-equilibrium effect. Such a wave is called a fully dispersed wave. The frozen Mach number M_f and the equilibrium Mach number M_e are noted as follows:

$$M_f = \frac{U_s}{a_f} = \frac{U_s}{\sqrt{\gamma_f RT}} \tag{13}$$

$$M_e = \frac{U_s}{a_e} = \frac{U_s}{\sqrt{\gamma_e RT}} \tag{14}$$

It is required that $M_f < 1$ and $M_e > 1$, to be a steady dispersed wave. However, the state of $M_f > 1$ exists in the unsteady process. The velocity of the shock wave U_s meets the following:

$$U_s > a_f \tag{15}$$

The discontinuous part, where the vibrational modes are frozen, is generated at the front of the shock wave, and the continuous profile generated by the vibrational modes is realized behind the shock front. Such a wave is called a partly dispersed wave. It is required to be a partly dispersed wave that $M_f > 1$.

Experimental setup

Experimental apparatus

Figure 2 shows a schematic diagram of our shock tube, which consists of a high pressure chamber and a low pressure chamber (glass shock tube). The low pressure chamber has an inner diameter of 1mm and a length of 600mm. The high pressure chamber, which has a simple structure, consists of a quickly opening valve using the rubber[6], a pressure chamber for the valve, and an outer diaphragm. High pressure air from a compressor is filled into the pressure chamber for the valve through a piping system and is monitored by a pressure gauge after controlling the pressure p_{valve}. Additionally, the quickly opening valve operates by manually bursting the outer diaphragm which is settled on the rear side of the pressure chamber. The pressures in the high pressure chamber for the shock tube and the low pressure chamber are denoted by p_4 and p_1, respectively. The pressure p_4 has to be kept lower than p_{valve} to separate the high pressure chamber from the low pressure chamber as the initial condition. The distance L^* between the quickly opening

valve and the measurement position is taken to 410mm. The driver gas is helium with the constant pressure p_4 and the test gas is CO_2 at different initial pressures p_1.

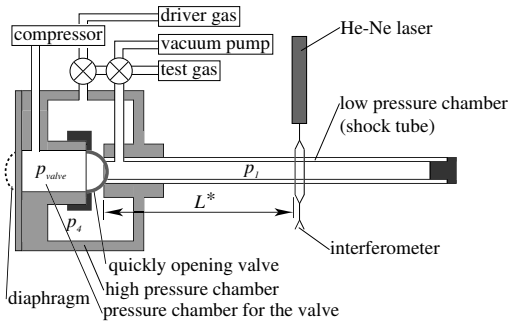

Figure 2: Schematic diagram of the small scale shock tube

Measurement system

The laser differential interferometric measurement method was developed by Smeets[7]. In particular, Smeets had developed the laser differential interferometer and measured the interferometric fringe image same as existing measurement method. However, the interferometer, which has a high resolution about hundredth part of the wave length for the change of the optical path difference, has been improved to measure the tone, which is observed in the interferometric fringe, by the photo diodes. For measuring the shock velocity and the density change caused by the shock wave, we used a specially designed laser differential interferometer set up by Wollaston prisms, which is based on the existing laser differential interferometer. The beam diameter is about several hundred micrometers for preventing optical curvature influences of the tube. The distance of the split beams is 5.59mm.

Results and discussion

Detection of the shock wave

Figure 3 shows the typical density trace of a normal shock wave structure in CO_2 obtained from the laser differential interferometer. The jump up of the signal is attributed to the fact that the propagating shock wave crosses into the first laser beam. The rapid falling down of the signal is attributed to the fact that the propagating shock wave crosses into the second laser beam. The distance between the initial jump up point and the rapid falling down point is the time difference of the laser differential interferometer. The shock wave velocity U_s and the density change ρ_2/ρ_1 can be calculated from the density trace. The partly dispersed wave is observed when the vibrational energy is frozen. The relaxation effect can be slightly seen in this figure. The thickness of the partly dispersed wave can also be calculated from the density trace. Figure 4 shows the typical density trace of the fully dispersed wave structure in CO_2, which is produced by the excitation of the vibrational energy, obtained from the laser differential interferometer. The interferometric signal seems very different from other figures for U_s=270m/s, because, before the jump up of the signal reaches the steady state, the rapid falling down of the signal is already coming. The fully dispersed wave velocity can be calculated from this density trace. However, calculating the density change is impossible on the density trace because of the same reason as mentioned before. At least, it is considered that the fully dispersed wave has the thickness of 5.59mm, or more. Figure 5 shows the typical density trace of the partly dispersed wave structure in CO_2 detected

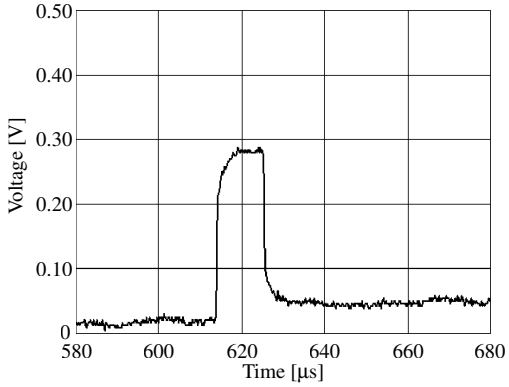

Figure 3: Density trace behind the shock wave in CO_2 driven by helium (p_4=2000mbar, p_1=50mbar, U_s=490m/s)

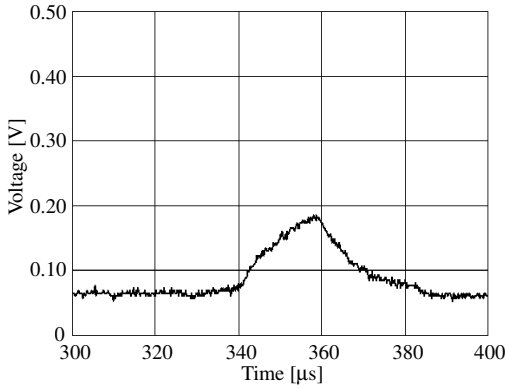

Figure 4: Density trace behind the shock wave in CO_2 driven by helium (p_4=1175mbar, p_1=400mbar, U_s=270m/s)

by the laser differential interferometer. Similarly, the partly dispersed wave velocity can be calculated from the density trace, but calculating the density change is impossible because that the drop down of the signal occurs before the increase of the signal reaching the steady state. It is also considered that the partly dispersed wave has the thickness over 5.59mm, only in the case where the shock wave velocity $a_e < U_s <$ 300m/s.

Classification of the dispersed wave by the shock velocity

Figure 6 shows the classification of the dispersed waves based on the shock wave velocity U_s from the experiments. The horizontal and vertical axes are the shock wave velocity U_s and the initial pressure ratio p_4/p_1. The pressure p_4 keeps a constant value for the different pressures p_1. Two vertical dashed lines correspond to the equilibrium sound velocity a_e and the frozen sound wave a_f, respectively. It is confirmed that the shock wave velocity, which has the fully dispersed wave shape, between a_e and a_f is presented by only one point in our experiments. The partly dispersed wave occurs at $a_f > U_s$.

The initial pressure ratio as a function of Mach number

The frozen specific heat is assumed that the vibrational modes are frozen, and the behaviour of CO_2 molecule is assumed to be the same as for the diatomic gas. However, it cannot describe the fully dispersed wave from the real polyatomic gas. Therefore, the assumption, that the vibrational mode is excited maintaining equilibrium with translational and rotational modes, should be referred for the calculation of the Mach num-

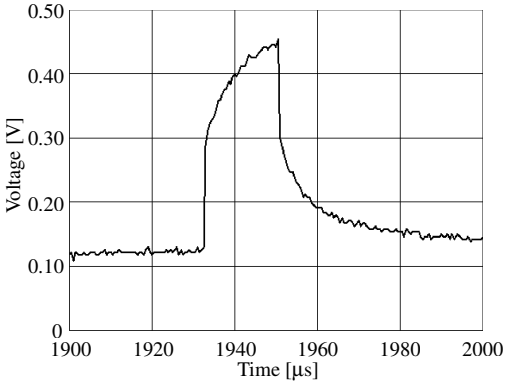

Figure 5: Density trace behind the shock wave in CO_2 driven by helium (p_4=1250mbar, p_1=390mbar, U_s=300m/s)

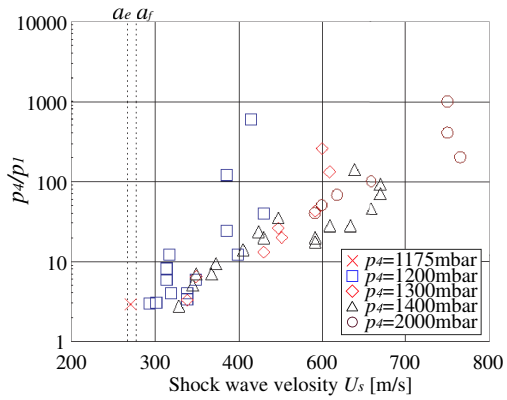

Figure 6: Classification of the dispersed wave by the shock velocity

ber of the fully or partly dispersed wave as in the following equation.

$$M_s = \frac{U_s}{a_e} = \frac{U_s}{\sqrt{\gamma_e RT}} \tag{16}$$

Figure 7 shows the Mach number of the fully or partly dispersed wave. The horizontal and vertical axes are the Mach number of the fully or partly dispersed wave M_s and the initial pressure ratio p_4/p_1. It is confirmed that the Mach number of the fully dispersed wave occurs in the very weak shock region, and the Mach number of the fully dispersed wave is M_s=1.012 in this case. It is expected that the pressure p_1 becomes important for the influence of the friction effects with smaller shock tubes. The Mach number increases with increasing the initial pressure ratio p_4/p_1, at least lower pressure p_1. Furthermore, figure 7 shows the very interesting result that the maximum Mach number occurs, and two different values of p_4/p_1 for the same Mach number M_s. It occurs at higher Mach number region as p_4 keeps constant with changing p_1.

Conclusions

The weak shock wave and the fully or partly dispersed wave have been produced in a small scale shock tube with a specially designed laser differential interferometer by using helium and CO_2 as driver and test gas as shown in figures 3, 4 and 5. It is possible to calculate the density change from the interferometric signals, but impossible in the case of the signals with dispersed wave. Similarly, the thickness of the fully or partly dispersed waves can be measured. However, it is not calculated because

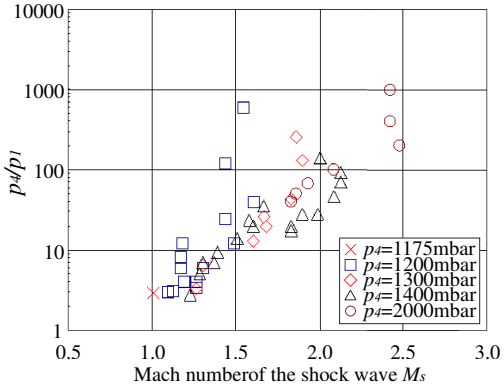

Figure 7: The Mach number of the fully or partly dispersed wave

the density jump does not arrive at steady states near M_s=1. The fully dispersed wave, which has the velocity U_s=270m/s, occurs between the equilibrium sound velocity a_e and the frozen sound velocity a_f. The maximum Mach number for the same pressure p_4 is strongly influenced, by the friction effects between the shock tube wall and the moving gas behind the shock wave. The higher p_4/p_1 value is combined with the smaller pressure p_1, and induced by a higher friction resistance, which again introduces two different pressure ratios p_4/p_1 for the same M_s.

Acknowledgements

The author would like to express his gratitude to the German Academic Exchange Service (DAAD). This project was performed during the first author's stay in Germany, financed by a scholarship from DAAD.

References

[1] Brouillette, M., Shock waves at micro scales, *Shock Waves*, **13**, 2003, 3–12.

[2] Garen, W., Buss, T., Foschepoth, S., Becker, M., Koch, S., Novoselova, E., A novel mini-shock tube for generating shock waves at micro scales in turbulent and laminar gas flows, *Proc. of 25th Int. Symposium on Shock waves*, 2005, 746–750.

[3] Udagawa, S., Maeno, K., Golubeva, I., Garen, W., Interferometric signal measurement of shock waves and contact surfaces in small scale shock tube, *Proc. of 26th Int. Symposium on Shock waves*, 2007 to be appeared.

[4] Garen, W., Meyerer, B., Udagawa, S., Maeno, K., Shock waves in mini-tubes: Influences of the scaling parameter *S*, *Proc. of 26th Int. Symposium on Shock waves*, 2007 to be appeared.

[5] Johannesen, N.H. and Hodgson, J.P., The physics of weak waves in gases, *Report on Progress in Physics*, **42**, 1979, 629–676.

[6] Garen, W., Synofzik, R., Frohn, A., Shock tube for generating weak shock waves, *AIAA Journal*, **12**, 1974, 1132–1134.

[7] Smeets, G., Laser interferometer for Transient Phase Objects, *Proc. of the eighth International Shock Tube Symposium*, 1971.